

1 **Variation in antiviral immunity and inflammation pathways**
2 **precedes HIV-1 infection in a high-risk African cohort**

3 Mwikali Kioko^{1*}, Shaban Mwangi¹, Lynn Fwambah¹, Amin S. Hassan^{1,2},
4 Jason T. Blackard³, Philip Bejon^{1,4}, Eduard Sanders^{5,6}, Thumbi
5 Ndung'u^{7,8,9,10}, Eunice W. Nduati^{1,4,11†}, Abdirahman I. Abdi^{1,4,11†}

6 ¹Bioscience Department, Kenya Medical Research Institute-Wellcome
7 Trust Research Programme, Kilifi, Kenya

8 ²Institute for Human Development, Aga Khan University, Nairobi, Kenya

9 ³Division of Gastroenterology & Hepatology, University of Cincinnati
10 College of Medicine, Cincinnati, Ohio, USA

11 ⁴Centre for Tropical Medicine and Global Health, Nuffield Department of
12 Medicine, University of Oxford, Oxford, UK

13 ⁵Sir William Dunn School of Pathology, University of Oxford, Oxford, UK

14 ⁶The Aurum Institute, Johannesburg, South Africa

15 ⁷Africa Health Research Institute, Durban, South Africa

16 ⁸HIV Pathogenesis Programme, The Doris Duke Medical Research
17 Institute, University of KwaZulu-Natal, Durban, South Africa

18 ⁹Ragon Institute of Mass General Brigham, Massachusetts Institute of
19 Technology and Harvard University, Cambridge, MA, USA

20 ¹⁰Division of Infection and Immunity, University College London, London,
21 UK

22 ¹¹Pwani University Biosciences Research Centre, Pwani University, Kilifi,
23 Kenya

24 *To whom correspondence should be addressed: Mwikali Kioko: P.O Box
25 230-80108, Kilifi, Kenya, +254711776932, [kmwikali@kemri-](mailto:kmwikali@kemri-wellcome.org)
26 wellcome.org

27 †These authors share senior authorship.

28 **Conflict-of-interest**

29 The authors have declared that no conflict of interest exists.

30 **ABSTRACT**

31 **Background**

32 Susceptibility to human immunodeficiency virus type 1 (HIV-1) infection
33 varies between individuals, but the biological determinants of acquisition
34 risk remain poorly defined.

35 **Methods**

36 We conducted a case-control study nested within a high-risk cohort in
37 Kenya. We compared the plasma extracellular RNA collected before
38 HIV-1 acquisition with matched uninfected controls to identify
39 immunological processes linked to infection risk.

40 **Results**

41 Individuals who later acquired HIV-1 exhibited upregulation of immune
42 processes that facilitate viral infection, including T cell suppression, type
43 II interferon and Th2 immune responses. In contrast, processes
44 associated with antiviral defence and tissue repair, such as neutrophil
45 and natural killer cell responses, type I interferon responses, wound
46 healing, and angiogenesis, were downregulated.

47 **Conclusion**

48 These findings highlight dampened antiviral immunity prior to exposure
49 as a correlate of increased risk for subsequent HIV-1 acquisition.

50 **Trial number**

51 Not applicable

52 **Funding**

53 This work was supported by a Wellcome Trust Award (209289/Z/17/Z)
54 and the Sub-Saharan African Network for TB/HIV Research Excellence
55 (SANTHE) through the DELTAS Africa programme [Del-22-007],
56 supported by the Science for Africa Foundation, Wellcome Trust, the UK
57 Foreign, Commonwealth & Development Office, and the European
58 Union. Additional support was provided by the Bill & Melinda Gates
59 Foundation, Gilead Sciences Inc., Aidsfonds, and the Ragon Institute of
60 Mass General, MIT, and Harvard. The cohort study was supported by
61 PEPFAR through USAID. The views expressed are those of the authors.

62

63

64

65

66

67

68

69 INTRODUCTION

70 Susceptibility to human immunodeficiency virus 1 (HIV-1) infection
71 varies significantly across populations and individuals (1-3). For
72 example, analysis from multiple studies showed that sub-Saharan Africa
73 has a higher risk of HIV-1 transmission per sexual contact compared to
74 higher-income regions (1). Although these differences may reflect low
75 access to antiretroviral drugs in sub-Saharan Africa at the time, intra-
76 population differences in susceptibility have been documented in a
77 longitudinal study of high-risk Kenyan adults, in which only 7% were
78 infected during follow-up despite likely widespread exposure (4). This
79 variability stems from a diverse range of factors, including behavioural
80 differences, viral load, characteristics of circulating viruses (including
81 HIV-1 subtype), and host-related factors such as genetic diversity and
82 environmental exposures such as sexually transmitted infections (STIs)
83 that can modulate basal immune status (2, 5, 6). However, the specific
84 host biological factors and pre-existing pathogens associated with HIV-
85 1 acquisition are not fully known.

86 Identifying biological determinants of HIV-1 susceptibility is crucial for
87 developing diagnostic biomarkers and interventions (7, 8). High-
88 throughput omic techniques, including proteomics and transcriptomics,

89 are increasingly employed to understand host mechanisms predisposing
90 to HIV-1 infections (4, 9). Transcriptomics offers a sensitive method to
91 detect subtle differences in gene expression, providing insights into the
92 host's immune response and immunomodulatory pathogens (10).

93 All cells secrete a diverse population of RNA collectively called
94 extracellular RNAs (exRNAs) into biofluids such as plasma, saliva, and
95 urine (11, 12). The majority of these exRNAs are secreted within
96 membrane-bound vesicles called extracellular vesicles (EVs), which
97 protect them in the harsh extracellular space (11-18). Additionally, the
98 profiles of circulating exRNAs largely reflect the biological state of the
99 secreting cells, which provides a more holistic view of systemic biological
100 processes (19-21) and pathogen signals (22-26) relative to the cellular
101 RNA obtained from peripheral immune cells. Therefore, analyzing
102 plasma-derived exRNA from pre-infection samples may provide valuable
103 immune correlates of HIV-1 acquisition.

104 Here, we highlight transcriptional immune correlates of HIV-1
105 susceptibility by retrospectively analysing plasma-derived exRNA
106 collected before HIV-1 infection in a case-control study nested within a
107 longitudinal cohort of HIV-negative high-risk individuals in coastal Kenya
108 (27).

109 RESULTS

110 Plasma exRNA highlights immunological pathways associated with 111 HIV-1 acquisition risk

112 The primary objective of this study was to identify pre-infection
113 transcriptional correlates of HIV-1 acquisition in high-risk adults. To
114 achieve this, we took advantage of a long-term longitudinal cohort of
115 high-risk individuals on the Kenyan coast, for whom the dates of HIV
116 infection have previously been estimated (4, 27-29) as summarised in
117 Figure 1 and described in detail in the Methods. We compared plasma-
118 derived exRNA from individuals who later acquired HIV-1 (cases; n=32),
119 collected approximately 3 ± 2 months prior to the estimated date of
120 infection, to that from matched negative controls (n=64) (Figure 1). This
121 analysis identified 767 genes with differentially increased abundance
122 and 774 genes with significantly decreased abundance in HIV-1 cases
123 at a false discovery rate (FDR) of less than 5% (Figure 2A). Next, we
124 performed principal component analysis (PCA) and supervised heatmap
125 clustering on the differentially enriched genes and found that the
126 transcriptional profiles of EVs distinguished controls from the HIV-1
127 cases (Figure 2B, C). The differentially increased genes included the
128 endothelial nitric oxide synthase (*NOS3*), angiotensin-converting

129 enzyme 2 (*ACE2*), interleukin 17 and 21 receptors (*IL17RA*, *IL17RD*,
130 *IL21R*), the viral-sensing Toll-like receptor 7 (*TLR7*), and the inhibitor of
131 *IRF3*- and NF- κ B-dependent antiviral response gene (*ILRUN*) (30)
132 (Figure 2C). In contrast, the differentially decreased genes featured the
133 pro-angiogenic factor *VEGFA*, the interferon regulatory factors (*IRF1*,
134 *IRF3*, *IRF4*, and *IRF5*), and the p53 negative regulator *MDM2* (Figure
135 2C).

136 Cell enrichment analysis demonstrated that the genes upregulated in
137 HIV-1 cases 3 \pm 2 months prior to infection belonged to cells such as
138 eosinophils, plasma B cells, central memory CD8-T cells, plamacytoid
139 dendritic cells (pDCs), and Th2 cells (Figure 2D). In contrast, the
140 downregulated genes were enriched for signatures associated with
141 several cell types, including natural killer (NK) cells, B-memory cells, and
142 neutrophils (Figure 2D). Next, we performed pathway enrichment
143 analysis of the 767 genes increased in HIV-1 cases, revealing an
144 overrepresentation of genes linked to endothelial nitric oxide synthase
145 (eNOS), IL-17 and IL-10 signalling, suppressive T-cell response, and
146 apoptosis (Figure 2E). Conversely, the 774 genes decreased in HIV-1
147 cases belonged to a wide range of biological pathways, including
148 reparative processes (wound healing and p53-signalling pathway) and

149 pathways related to type-I interferon (IFN), including NF κ B activation by
150 protein kinase R (PKR) and IFN-beta signalling (Figure 2E). These
151 findings suggest that reduced type I interferon and pro-reparative
152 immune responses, alongside elevated eNOS, suppressive T cell
153 response, IL17 and IL10 signalling, are strongly linked to HIV-1
154 acquisition in high-risk adults.

155 **Plasma exRNA clustering uncovers distinct immunological** 156 **endotypes in HIV-1 cases and controls.**

157 There could be heterogeneity in the biological mechanisms that underlie
158 protection or susceptibility to HIV-1 infection, which is obscured when
159 comparing the average biological signals between cases and controls.
160 To reveal intragroup heterogeneity and biological signal, we constructed
161 a participant similarity network (PSN) using the exRNA dataset
162 generated from the samples collected 3 ± 2 months prior to HIV-1
163 infection. Spectral clustering of the similarity network identified five
164 endotypes of study participants - named A, B, C, D, and E - of which
165 endotypes A, B, and C were enriched for controls, while D and E were
166 enriched for HIV-1 cases (Figures 3A-C). We subsequently performed
167 differential feature analysis and identified over 4000 genes whose
168 exRNA profiles differed significantly between the endotypes, surpassing

169 the differential signal observed in the case-control analysis (Figure 3D,
170 Supplemental Table 1). Pathway enrichment analysis revealed that the
171 control endotypes were enriched for features associated with pro-
172 reparative processes (wound healing, TGF-beta/SMAD signalling,
173 VEGF overexpression and histamine metabolism), T cell function (T cell
174 CD3, T cytotoxic cell surface, co-stimulatory T cell activation, granzyme-
175 B pathway and CTLA4 signalling), mitochondrial function (protection
176 against ROS, Keap1-Nrf2, respiratory electron transport, citric acid
177 cycle), and type I IFN signalling (IFN Beta signalling pathway, cGAS-
178 STING-TBK1 pathway, TLR-TRIF pathway, NFkB activation by PKR)
179 (Figure 3E).

180 The two endotypes composed mainly of HIV-1 cases (Figure 3A-C) were
181 also enriched for distinct pathways, with genes augmented in endotype
182 D featuring those linked to eNOS signalling, regulatory T cells, CXCR4
183 signalling, and FAS-mediated apoptosis (Figure 3E). Finally, endotype E
184 showed evidence of increased apoptosis, including HIV-1 mediated T
185 cell apoptosis, TRAIL and DR3 death receptor signalling. Signatures of
186 B-cell differentiation, IL-7 signalling, and suppressor of cytokine
187 signalling (SOCS) were also enriched in endotype E (Figure 3E). Our
188 endotyping analysis revealed more differentially expressed genes, and

189 enrichment analysis compared to case-control analysis, which suggests
190 that different biological mechanisms could promote or impede HIV-1
191 infection.

192 **The immunological processes observed at 3±2 months were**
193 **conserved at 6±2 months prior to HIV-1 infection.**

194 To investigate whether the immune profile observed 1 to 5 months prior
195 to HIV-1 infection was also evident at earlier time points, we analysed
196 the transcriptional profiles from 9 individuals who later acquired HIV-1
197 and 29 matched controls who remained uninfected, using samples
198 collected 4 to 8 months before the cases became HIV-1 positive. We
199 found that 2688 genes were significantly increased in HIV-1 cases, while
200 4521 genes were significantly decreased (Figure 4A, Supplemental
201 Table 2). Cellular enrichment analysis of the altered genes showed
202 significant downregulation of genes belonging to natural killer cells (e.g.
203 *NCAM1*, *FCGR3A*), plasma B-cells (e.g. *CD38*), and pDCs (Figure 4A-
204 B). When we performed pathway over-representation analysis, we
205 observed that genes upregulated 6±2 months prior to HIV-1 infection
206 featured those belonging to type II interferon signalling (e.g. *CXCR3*,
207 *IFNG*, *IL19*, and *CXCL9*) (Figure 4C). On the other hand, genes
208 downregulated 6±2 months prior to HIV-1 infection were enriched for

209 type I interferon signalling (e.g. *IRF3*, *IRF9*, *JAK1*, *STAT2*, *STAT5A*,
210 *IL1B*, *TLR2*, *TLR4*), and VEGFA-VEGFR2 signalling, consistent with the
211 3±2 months prior to infection timepoint (Figure 4C). These observations
212 confirm that reduced type 1 interferon-driven innate immunity, together
213 with an elevated type II interferon state, precedes HIV-1 infection.

214 **The presence of human pegivirus type-1 (HPgV-1) is associated**
215 **with HIV-1 acquisition.**

216 We next analyzed the exRNAseq data using a metatranscriptomic
217 approach to nominate potential pathogens associated with HIV-1
218 susceptibility. HPgV-1 RNA abundance was significantly higher in HIV-1
219 cases than controls three months before HIV infection (\log_2 fold-
220 change>4, FDR<0.05) but not at six months (Figure 5A). Applying more
221 stringent criteria (>5 reads) to define HPgV1 positivity, rather than
222 considering any detectable HPgV1 RNA level as positive, we identified
223 20 HPgV1 positives. HPgV-1 positivity was non-significantly higher
224 among HIV-1 cases than controls at both three months (28% in cases
225 versus 17% in controls; OR = 1.89, 95% CI 0.69-5.16, p = 0.29) and at
226 six months (22% in cases versus 14% in controls; OR = 1.79, 95% CI
227 0.27-11.86, p = 0.61, indicating a modest enrichment of HPgV1 among
228 individuals who later acquired HIV-1 (Figure 5B). 14 participants were

229 identified as HPgV-1 positive by conventional PCR, of which only 3 of
230 them were not detected using NGS. (Figure 5C). Poisson regression
231 analyses showed that HPgV-1 infection detected by next-generation
232 sequencing (NGS) and PCR at 3 ± 2 months prior to HIV-1 infection was
233 significantly associated with HIV-1 acquisition (NGS: RR = 1.99, 95% CI
234 1.11-3.55; PCR: RR = 2.32, 95% CI 1.32-4.08) (Figure 5D). However,
235 after adjustment for other sexually transmitted infections, the association
236 was reduced (NGS: RR = 1.51, 95% CI 0.88-2.61; PCR: RR = 1.66, 95%
237 CI 0.96-2.87), indicating that HPgV-1 was not an independent predictor
238 of HIV-1 acquisition. We next compared the endotypes by HPgV1 status,
239 revealing that individuals clustered in endotype D were more likely to be
240 HPgV1 positive compared to endotypes A or B (Figure 5E). To assess
241 the impact of HPgV-1 on transcriptional alterations between HIV-1 cases
242 and controls, we compared the transcriptional difference between HIV-1
243 cases and controls, before and after adjusting for HPgV-1 status. We
244 found a high correlation ($R=0.97$, $P<0.0001$) of the \log_2 fold changes
245 before and after adjusting for HPgV1 (Figure S1, Supplementary Table
246 3). Further, 120 and 201 of the upregulated and downregulated genes
247 between HIV-1 cases and controls, respectively, showed significant
248 differential abundance between HPgV-1 positive and negative
249 individuals (Figure S2, Supplementary Table 4). We also compared

250 transcriptional changes between HPgV1-positive and -negative
251 individuals within both the HIV cases and the control groups and found
252 overlaps of 37 (3.7%) and 38 (4.8%) upregulated and downregulated
253 genes, respectively (Figure S3; Supplementary Table 5). Additionally, we
254 reanalysed previously published transcriptional data from PBMCs that
255 were either exposed or unexposed to HPgV1 *in vitro*. The reanalysis
256 revealed only 12 genes (6 upregulated and 6 downregulated) with
257 concordant expression between exRNA and PBMCs (Figure S4 and
258 Supplementary Table 6).

259 Finally, we assessed the genetic relatedness of the HPgV-1 genome
260 sequences from the 3 ± 2 months prior to infection samples relative to
261 those from other parts of the world. We generated 11 partial HPgV-1
262 genomes, of which 4 were from the controls and 7 were from the HIV-1
263 cases. We next performed phylogenetic analysis and found that the
264 HPgV-1 genomes clustered by geographic origin, with our partial
265 genomes co-clustering with those from other African countries,
266 consistent with previous studies(31) (Figure 5F).

267

268

269

DISCUSSION

In this study, we leveraged plasma-derived exRNA to determine pre-infection immune correlates of HIV-1 acquisition among high-risk adults in a longitudinal cohort study (27, 29). We highlight key findings, explore their biological relevance to HIV-1 susceptibility, and offer potential avenues for future research and intervention. Given that the profiles of circulating exRNA often mirror molecular activities in the tissues most affected by a specific condition (32), in this case, the mucosal sites that serve as primary portals of HIV-1 entry, we also discuss our observations within the context of mucosal immune regulation.

Our differential feature analysis showed that, three months prior to HIV-1 infection, individuals who later got infected exhibited significant alterations in exRNA profiles compared to the controls. Notably, transcripts associated with IL-17 receptor signalling, apoptosis, regulatory T-cells, and eNOS signalling were upregulated in HIV-1 cases. Higher sexual activity, particularly receptive anal intercourse (33-35), together with STIs, may promote mucosal damage, immune activation and apoptosis, events that compromise barrier integrity and facilitate viral entry. The elevated IL-17 receptor and eNOS signalling, along with Treg responses, may represent compensatory mechanisms

290 that restore mucosal homeostasis (36-43) but could also be induced by
291 STIs and anal intercourse (33, 44). However, chronic activation of these
292 pathways could sustain inflammation and tissue damage. Moreover,
293 enhanced IL-17 receptor signalling may also drive chemokines that
294 enhance Th17 cell recruitment at mucosal sites (45), key HIV-1 target
295 cells (46-48). While Tregs help reduce immune activation, they are also
296 susceptible to HIV-1 infection (49, 50) and can weaken antiviral
297 response, collectively enhancing susceptibility to HIV-1 acquisition.

298 A key observation from our study was the downregulation of genes linked
299 to type I interferon response, accompanied by an upregulation of type II
300 interferon-associated transcripts in individuals who later acquired HIV-1.
301 This pattern suggests a reprogramming of the immune landscape toward
302 a less antiviral (30, 51-57) and more inflammatory state, which may
303 increase the expression of key HIV-1 entry receptors such as CCR5 (58-
304 60), thereby increasing susceptibility to HIV-1 infection. The
305 suppression of type I interferon response may be driven by elevated IL-
306 17 signalling, given that type I interferon and Th17 responses are known
307 to act antagonistically (61). Indeed, individuals with a gain-of-function
308 mutation in type 1 interferon signalling are predisposed to fungal
309 infection due to impaired Th17 responses (62, 63), while chronic

310 hyperactivation of Th17 responses has been associated with increased
311 susceptibility to viral infections (45, 64, 65).

312 Our endotyping analysis identified five distinct endotypes, reflecting
313 significant heterogeneity in the biological mechanisms at play. Three
314 endotypes - A, B, and C -predominantly comprising controls, displayed
315 immune profiles consistent with effective antiviral immunity (66, 67) and
316 restrained immune activation, characterised by enhanced type I
317 interferon response, T-cell function, TGF-beta/SMAD signalling, and
318 oxidative phosphorylation. These features likely contribute to efficient
319 antiviral defence (57) and maintenance of mucosal health. For example,
320 increased TGF-beta could confer protection against HIV-1 infection
321 through maintaining an effective mucosal immune system impervious to
322 viral entry (68, 69) or inhibiting the pro-HIV type II IFN immune response
323 (70). In contrast, the two susceptibility endotypes, D and E, were
324 enriched for regulatory T-cells and FAS-mediated signalling, TRAIL, and
325 SOC3 pathways, signatures that suppress antiviral immunity and
326 enhance mucosal disruption (71-73). Together, these findings suggest
327 that pre-infection immune heterogeneity, particularly involving interferon
328 balance and T-cell function interplay, critically shapes HIV-1 acquisition

329 risk and may inform precision prevention strategies. However, a larger
330 study is necessary to identify the true heterogeneity of HIV-1 risk.

331 Our metatranscriptomic analysis identified HPgV-1 (also called human
332 pegivirus C type 1 or GB virus C [GBV-C] or *Pegivirus hominis*) as
333 significantly associated with HIV-1 acquisition, albeit less pronounced
334 when adjusting for other STIs. HPgV-1 is a flavivirus that infects
335 lymphocytes and NK cells and is transmitted by blood transfusion,
336 sexual exposure, and mother-to-fetal transmission (74). While our data
337 suggests that HPgV-1 is a correlate of HIV-1 acquisition, its predictive
338 value is influenced by the presence of other STIs. This suggests that
339 HPgV-1 may not directly drive susceptibility but instead reflects a
340 permissive host immune environment conducive to sexually transmitted
341 viral infection, thus representing a biomarker for HIV-1 risk.

342 Interestingly, during established HIV-1 infection, HPgV-1 has been linked
343 to slower progression to acute immunodeficiency syndrome (AIDS) (75-
344 79). A plausible explanation, which is consistent with our data, is that
345 HPgV-1 exploits an immune milieu characterised by reduced type I and
346 elevated type II interferon response (80), an immune balance that
347 favours viral acquisition but limits immunopathology (81-84). However,

348 a direct role for HPgV-1 in modulating host immunity cannot be ruled out,
349 as suggested by other studies (26, 85-87).

350 The retrospective design of our study represents a key limitation.
351 Concurrent collection of mucosal samples alongside blood would have
352 allowed direct validation of the immunological signatures inferred from
353 exRNA analyses against local mucosal responses. Consequently, some
354 of our interpretations, although supported by existing literature, remain
355 speculative and require confirmation through prospective studies.

356 In summary, we highlight the strength of plasma exRNAseq in
357 uncovering pre-infection biological correlates of HIV-1 acquisition.
358 Future research should focus on validating the predictive value of HPgV-
359 1 in larger cohorts and exploring its utility in predictive models and
360 targeted interventions. In conclusion, understanding the biological
361 drivers of HIV-1 susceptibility among high-risk populations could
362 enhance the development of prevention and treatment strategies.

363

364

365

366

367 **METHODS**

368 **Sex as a biological variable**

369 Samples from cases and controls were obtained from both men and
370 women. In our study, sex was not considered a biological variable of
371 interest.

372 **Study design and population**

373 *3±2 months prior to HIV-infection samples:* A case-control study nested
374 in a historic HIV-1 high-risk cohort from Coastal Kenya was conducted.
375 HIV-1 negative high-risk volunteers, including men-who-have-sex-with-
376 men (MSM) and female sex workers (FSW) aged ≥18 years, were
377 recruited and followed from 2006 to 2011 for HIV-1 vaccine
378 preparedness studies. Volunteers were screened for incident HIV-1
379 infection during follow-up using RT-PCR, p24 antigen, and HIV-1-
380 specific antibody assays as previously described (4, 28). For any
381 volunteer testing HIV-1 positive, an estimated date of infection (EDI) was
382 calculated either to be: 10 days before a positive HIV-1 RNA test (if
383 antibody negative), 14 days before a p24 antigen positive test (if RNA
384 test was missing), or midway between the last negative and first positive
385 HIV-1 specific antibody test (if both RNA and p24 tests were missing).
386 Cases were defined as volunteers who tested HIV-1 positive, while

387 controls were those who remained negative at the end of a similar follow-
388 up period (4). Plasma samples from cases were collected 3 ± 2 months
389 prior to the EDI, with controls matched 2:1 to cases based on sex, age,
390 risk group, follow-up duration, and plasma sample availability.

391 *6±2 months prior to HIV infection samples:* Plasma samples collected
392 6 ± 2 months before the EDI were retrieved. Controls were matched 2:1
393 to HIV cases based on age, sex, risk group, follow-up duration in the
394 study and the availability of plasma samples collected at around the
395 same calendar date as that of the index case ± 2 months.

396 **Isolation of extracellular RNA**

397 Nanofiltration and ultracentrifugation were used to isolate exRNA,
398 aiming to primarily enrich for those encapsulated in small EVs, as
399 described previously (19) In brief, 13.5 ml of prefiltered PBS was
400 combined with 300 μ L of plasma in a 15 ml Falcon tube. The diluted
401 plasma was filtered through a 0.22 μ m (Millipore) filter to exclude cell
402 debris and centrifuged at 150,000 x g for 2 hours at 4 °C without
403 breaks. The pellets were treated with RNase A for 15 min and washed
404 at 150,000 x g for two hours at 4°C. The impact of the RNase treatment
405 was evaluated by comparing the exRNA profile before and after
406 treatment using bioanalyzer/Agilent TapeStation (Figure S5). The

407 supernatant was discarded while the pellets were digested using 250 μ l
408 of RNA lysis solution (Bioline) and stored at -80°C until needed. ExRNA
409 was extracted from the lysed pellets using the Isolate II RNA Mini Kit
410 (Bioline) as directed by the manufacturer.

411 **Bead-assisted flow cytometry**

412 Evaluation of small EV markers in our pellets was performed using bead-
413 assisted flow cytometry (Figure S5), as we previously described (88).
414 Briefly, 50 μ L of EVs in PBS were incubated with 1 μ L of aldehyde/sulfate
415 latex beads (Invitrogen) in a total volume of 1 mL PBS for 12 hours at
416 room temperature on a rotary mixer. Following incubation, 110 μ L of 1 M
417 glycine was added to block unreacted sites, and the mixture was
418 incubated for an additional 30 minutes at room temperature. Beads were
419 pelleted by centrifugation at $2000 \times g$ for 5 minutes and washed once
420 with 1 mL PBS. The pellet was resuspended in PBS supplemented with
421 0.5% fetal bovine serum (PBS + 0.5% FBS) and stained with $1\times$ anti-
422 CD9-APC (Cat. No. 341648, BD Biosciences) and $1\times$ anti-CD63-PE
423 (Cat. No. 55705, BD Biosciences). Negative controls included beads
424 incubated with (i) antibody cocktail without EVs, and (ii) isotype control
425 antibodies: PE mouse IgG1 (Cat. No. 556650, BD Biosciences) and APC
426 mouse IgG1 (Cat. No. 550854, BD Biosciences). Stained beads were

427 washed twice with 500 μ L PBS + 0.5% FBS and pelleted by
428 centrifugation at 2000 $\times g$ for 10 minutes. Data acquisition was
429 performed using a BD Fortessa flow cytometer.

430 **cDNA library preparation**

431 We used our previous protocol(19, 88) to prepare the cDNA libraries for
432 sequencing. Briefly, Superscript III (Invitrogen) was used to produce the
433 first strand from the total exRNA. Before synthesizing the second strand,
434 the first strand reaction was cleaned using RNACleanXP beads. dTTP
435 was replaced with dUTP while synthesizing the second strand to
436 generate double-stranded cDNA. The cDNA was fragmented, end-
437 repaired and ligated to adapters. The cDNA was treated with USER
438 followed by 19 cycles of PCR amplification to add Illumina primers and
439 increase yield. Sequencing was performed using the NextSeq 550
440 genome analyzer.

441 **Quantification of HPgV-1 using PCR**

442 HPgV-1 RNA was converted to cDNA using Superscript III reverse
443 transcriptase (NEB). HPgV-1 positive samples were detected by
444 amplicon-targeted PCR amplification of the 5' untranslated region (UTR)
445 with the antisense primer 5' - ATG CCA CCC GCC CTC ACC CGA A -
446 3' (nucleotides [nt] 494-473 according to GenBank accession number

447 AY196904) and the sense primer 5' - AAA GGT GGT GGA TGG GTG
448 ATG - 3' (nt 67-87) using Q5[®] High-Fidelity DNA Polymerase (New
449 England Biolabs). Amplification conditions were 50°C for 59 minutes, 10
450 minutes at 94°C, then 35 cycles of 30 seconds at 94°C, 1 minute at 55°C,
451 and 1 minute at 72°C, followed by 20 minutes at 72°C. First-round
452 polymerase chain reaction (PCR) products were used in nested PCR
453 with the antisense primer 5' – CCC CAC TGG TCY TTG YCA ACT C -
454 3' (nt 362-341) and sense primer 5' – AAT CCC GGT CAY AYT GGT
455 AGC CAC T - 3' (nt 107-131). After 35 cycles of 30 seconds at 94°C, 30
456 seconds at 55°C, and 1 minute at 72°C, PCR products were visualized
457 by agarose gel electrophoresis for the presence of a 256 nt band.

458 **Statistics**

459 Gene body read coverage depicted in Figure S7 was calculated using
460 the *RSEQC* tool. Transcript quantities in the units of raw read counts and
461 transcripts per million (TPM) were estimated by aligning the data to the
462 human transcriptomes using *salmon* and *tximport*. Comparison between
463 cases and controls was performed using *edgeR*. Raw read counts were
464 normalized using the relative log expression (RLE) method, and the
465 likelihood ratio test was chosen. *P*-values were adjusted for multiple
466 testing using the Benjamini-Hochberg statistical procedure, and an FDR

467 threshold of less than 5% was set as the cut-off for significance.
468 Endotyping was conducted using spectral clustering, while differences
469 in gene expression between the endotypes were determined in *edgeR*
470 as described above. Cellular overrepresentation was performed using
471 protein signatures derived from a previously published study(89) while
472 pathway genesets were obtained from *Literature Lab*(90) and
473 *WikiPathway*(91). Pathogen classification was performed using Kraken2,
474 while a comparison of pathogen abundance between cases and controls
475 was performed using *edgeR*. In parallel, the predictive value of HPgV-1,
476 as measured by both sequencing and PCR, was also assessed by
477 calculating risk ratios, with or without adjustment of other STIs. HPgV-1
478 phylogenetic tree was generated by first performing multiple sequence
479 alignment using *nextalign* followed by tree reconstruction using *iqtree*.
480 Unless stated otherwise, all visualizations were carried out using *ggplot2*
481 and *ComplexHeatmap* R packages.

482

483

484

485

486 **STUDY APPROVAL**

487 The samples used in this study were collected using the IAVI protocol B,
488 reviewed by the Kenya Medical Research Institute Ethical Review
489 Committee. Participants provided their written informed consent.

490 **DATA AVAILABILITY**

491 This study did not produce unique reagents or materials. RNAseq data
492 have been deposited at GEO under the accession number GSE287060
493 (<https://www.ncbi.nlm.nih.gov/geo/query/acc.cgi?acc=GSE287060>).

494 Datapoint values for all graphs are available in the Supporting Data
495 Values file.

496 **AUTHOR CONTRIBUTIONS**

497 A.I.A. E.W.N. and T.N. jointly conceived the project and secured funding.
498 P.B. guided data analysis and review of the manuscript. E.S. designed
499 and ran the cohort and contributed to the study design and review of the
500 manuscript. L.F. and A.S.H. participated in the study design and sample
501 selection. M.K. and S.M. performed the laboratory experiments. M.K.
502 performed data analysis and wrote the initial draft. J.B. designed HPgV-
503 1 primers and assisted in project conception. A.I.A. and E.W.N. jointly
504 supervised the project. All authors read and reviewed the final draft.

505 **ACKNOWLEDGEMENT**

506 This research was supported by a Wellcome Trust Award (209289/Z/17/Z) and
507 the Sub-Saharan African Network for TB/HIV Research Excellence (SANTHE)
508 which is administered by the Africa Health Research Institute (AHRI) and funded
509 by the Science for Africa Foundation to the Developing Excellence in
510 Leadership, Training and Science in Africa (DELTAS Africa) programme [Del-
511 22-007] with support from Wellcome Trust and the UK Foreign, Commonwealth
512 & Development Office and is part of the EDCPT2 programme supported by the
513 European Union; the Bill & Melinda Gates Foundation [INV-033558]; Gilead
514 Sciences Inc., [19275], Aidsfonds [0454] and the Ragon Institute of Mass
515 General, MIT, and Harvard. The cohort study was conducted by IAVI with
516 support of the American People through the U.S. President's Emergency Plan
517 for AIDS Relief (PEPFAR) through United States Agency for International
518 Development (USAID). All content contained within is that of the authors and
519 does not necessarily reflect the positions or policies of the funders. For the
520 purpose of open access, the author has applied a CC BY public copyright
521 licence to any Author Accepted Manuscript version arising from this submission.
522 This manuscript is published with permission of the Director, KEMRI.

523

524

525

526 **SUPPLEMENTAL TABLES**

527 Supplemental Table 1: excel file containing additional data related to
528 Figure 3.

529 Supplemental Table 2: excel file containing additional data related to
530 Figure 4.

531 Supplemental Table 3: excel file containing additional data related to
532 Figures S1

533 Supplemental Table 4: excel file containing additional data related to
534 Figures S2

535 Supplemental Table 5: excel file containing additional data related to
536 Figures S3

537 Supplemental Table 6: excel file containing additional data related to
538 Figures S4

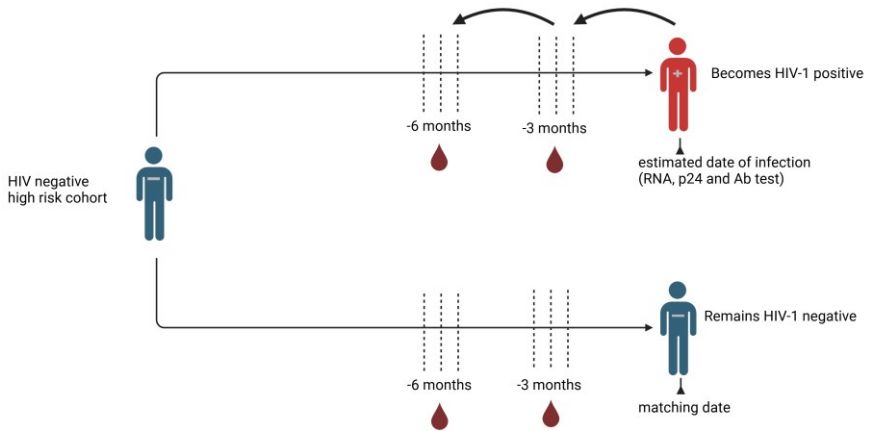
539

540

541

542

Figure and legends



544

545

546

547

548

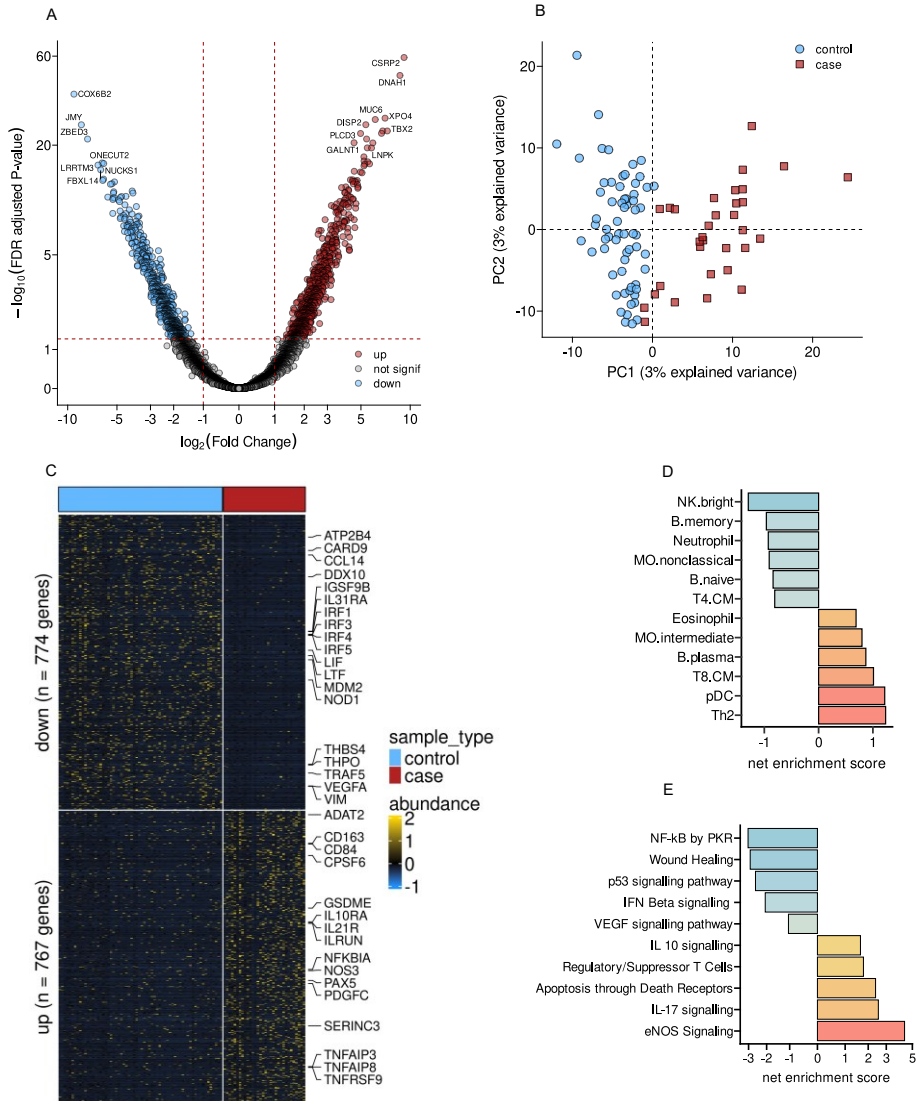
549

550

551

552

Figure 1: Schematic representation of our study design. Three and six-month prior to HIV infection, samples were selected from a historic high-risk cohort study conducted on the Kenyan coast between 2006 and 2011. Cases were defined as those who tested HIV positive during follow-up using RT-PCR, p24 antigen, and HIV-1-specific antibody assays. Controls were those who remained HIV-negative during follow-up and were matched to the cases based on sex, age, risk group, follow-up duration, and availability of samples.



553

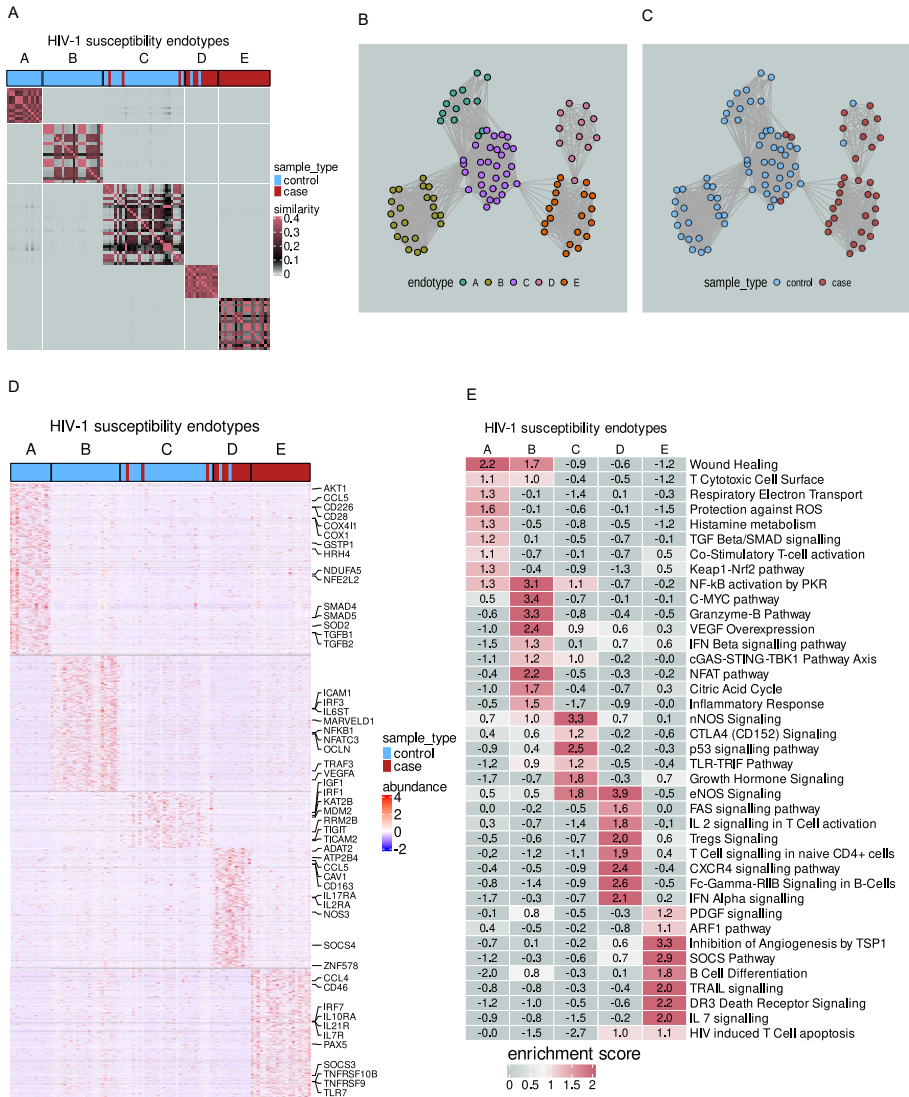
554

Figure 2: Cases exhibited a deregulated immunological profile

555

three months prior to HIV-1 infection

556 (A) Volcano plot showing differentially altered genes between 32 cases
557 and 64 controls, three months prior to cases being HIV positive. Red
558 dots represent genes upregulated in cases, blue represents
559 downregulated genes, and grey represents unaltered genes. (B) The
560 differentially altered genes can distinguish HIV-1 cases from those who
561 remained negative. (C) Supervised heatmap clustering showing
562 differences in gene expression between cases and controls. (D) Gene
563 enrichment analysis showing transcriptional alteration at the cellular
564 level. Genes belonging to neutrophils were downregulated, while those
565 belonging to eosinophils and memory Tregs (mTregs) were upregulated.
566 (E) Pathway gene enrichment analysis shows that immunosuppressive
567 biological processes, such as IL10 signalling and regulatory T cells, were
568 upregulated in the cases, while inflammatory and reparative processes
569 were downregulated.



570

571

Figure 3: Cases and controls cluster into distinct immunological

572

endotypes three months prior to HIV-1 infection

573 (A) Patient similarity matrix showing that EVs-RNAseq data, three
574 months prior to HIV-1 infection, splits controls and cases into three and
575 two endotypes, respectively. (B and C) Patient similarity network colored
576 by (B) endotype and (C) sample type. Each node represents a study
577 participant, and each edge links two similar samples. (D) Heatmap
578 clustering shows that the identified endotypes have distinct
579 transcriptional profiles. (E) Heatmap showing the top pathways enriched
580 in each endotype.

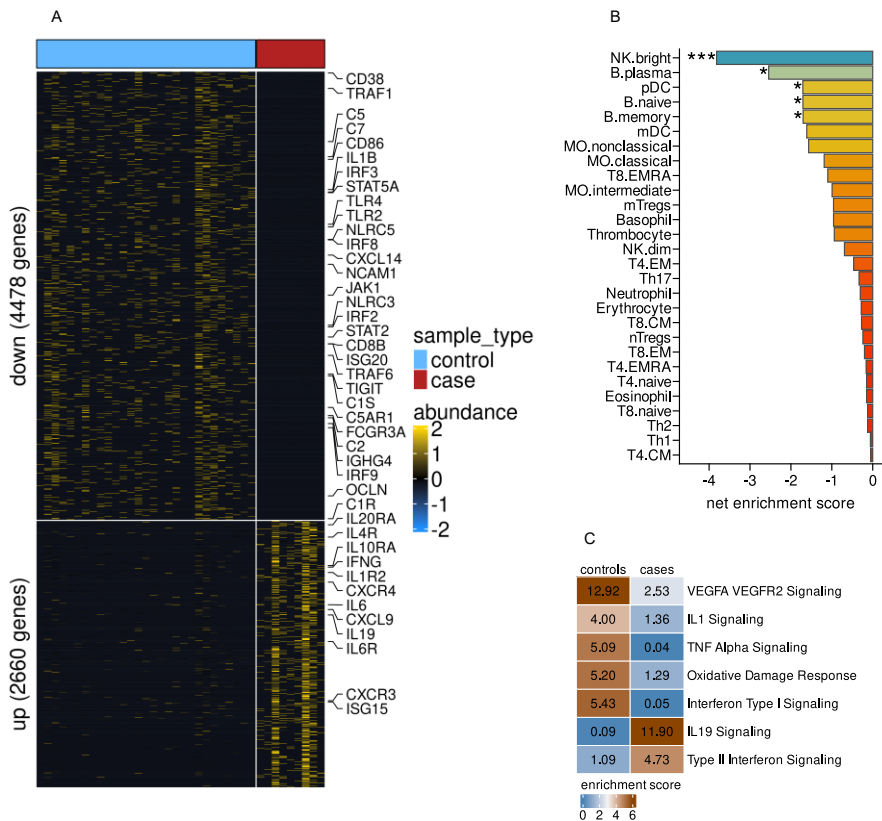
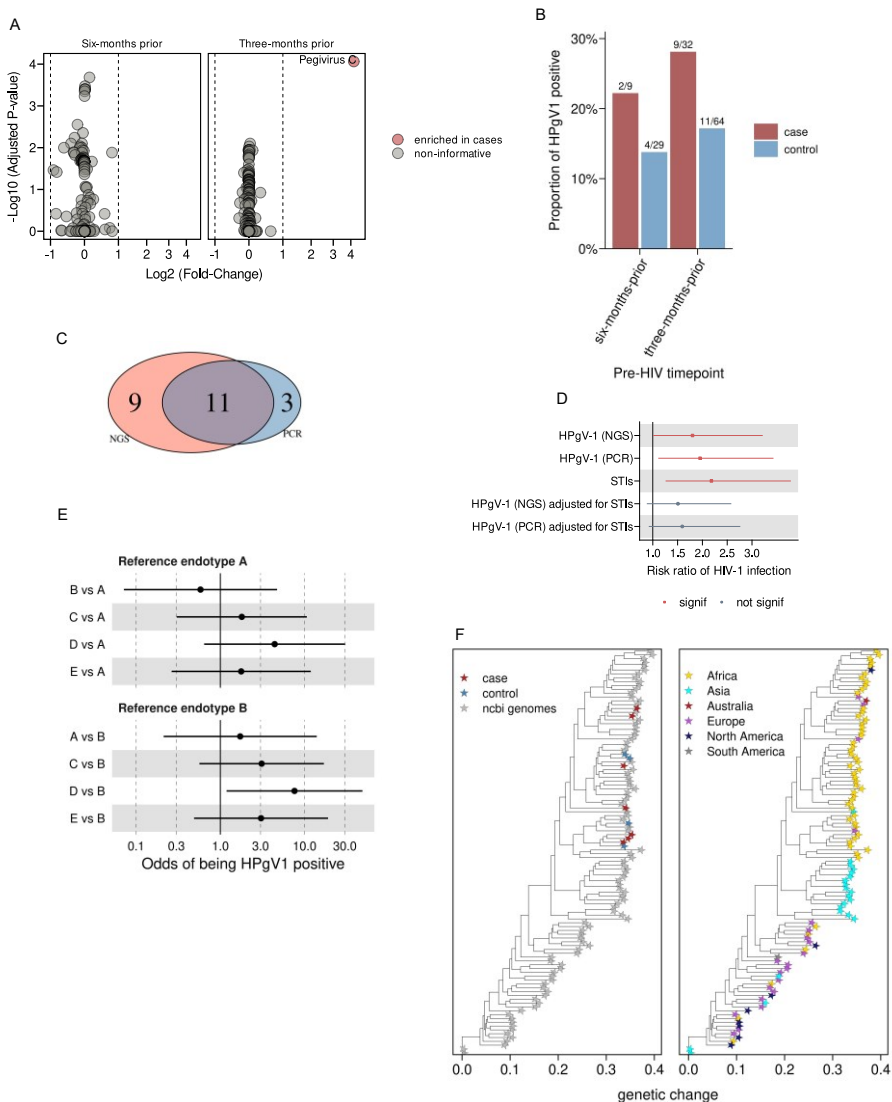


Figure 4: The immunosuppressive transcriptional profile is also evident six months prior to HIV-1 infection.

(A) Heatmap showing differential gene expression between 9 cases and 29 controls six months prior to HIV-1 infection. (B) Genes belonging to NK cells and plasma B-cell subsets are severely downregulated in HIV-1 cases relative to controls six months prior to infection. (C) Type II interferon response is upregulated in HIV-1 cases six months prior to infection, while type I interferon response pathways are upregulated.



590

591

Figure 5: HPgV-1 infection predicts HIV-1 acquisition.

592

(A) HPgV-1 RNA is more abundant in cases compared to controls at six

593

months prior to HIV-1 infection, but not at six months. (B) Barplots

594 showing the proportion of HPgV1 positive in HIV1 cases and controls.
595 **(C)** Venndiagram showing overlap of HPgV-1 detection using next-
596 generation sequencing (NGS) and conventional PCR. **(D)** The presence
597 of HPgV-1 three months prior to infection is a non-independent predictor
598 of HIV-1 infection. **(E)** Forest plots comparing HPgV1 status between the
599 endotypes described in Figure 2. **(F)** HPgV-1 genomes exhibit regional
600 clustering.

601

- 603 1. Boily MC, Baggaley RF, Wang L, Masse B, White RG, Hayes RJ, et al.
604 Heterosexual risk of HIV-1 infection per sexual act: systematic
605 review and meta-analysis of observational studies. *Lancet Infect*
606 *Dis.* 2009;9(2):118-29.
- 607 2. Lama J, and Planelles V. Host factors influencing susceptibility to
608 HIV infection and AIDS progression. *Retrovirology.* 2007;4:52.
- 609 3. Marmor M, Hertzmark K, Thomas SM, Halkitis PN, and Vogler M.
610 Resistance to HIV infection. *J Urban Health.* 2006;83(1):5-17.
- 611 4. Fwambah L, Andisi C, Streatfield C, Bromell R, Hare J, Esbjörnsson
612 J, et al. Exposure to common infections may shape basal immunity
613 and potentially HIV-1 acquisition amongst a high-risk population in
614 Coastal Kenya. *Front Immunol.* 2023;14:1283559.
- 615 5. Nigat AB, Abate MW, Demelash AT, Bantie B, Tibebe NS, Tiruneh
616 CM, et al. Predictors of HIV/AIDS preventive behavior among
617 undergraduate health science university students in Northwest
618 Ethiopia, 2022. Institution-based cross-sectional study. *Heliyon.*
619 2024;10(11):e32453.
- 620 6. Santos Í M, da Rosa EA, Gräf T, Ferreira LG, Petry A, Cavalheiro F, et
621 al. Analysis of Immunological, Viral, Genetic, and Environmental
622 Factors That Might Be Associated with Decreased Susceptibility to
623 HIV Infection in Serodiscordant Couples in Florianópolis, Southern
624 Brazil. *AIDS Res Hum Retroviruses.* 2015;31(11):1116-25.
- 625 7. Hulse SV, Antonovics J, Hood ME, and Bruns EL. Host-pathogen
626 coevolution promotes the evolution of general, broad-spectrum
627 resistance and reduces foreign pathogen spillover risk. *Evol Lett.*
628 2023;7(6):467-77.
- 629 8. Pirrone V, Mell J, Janto B, and Wigdahl B. Biomarkers of HIV
630 Susceptibility and Disease Progression. *EBioMedicine.* 2014;1(2-
631 3):99-100.
- 632 9. Grabowska K, Harwood E, and Ciborowski P. HIV and Proteomics:
633 What We Have Learned from High Throughput Studies. *Proteomics*
634 *Clin Appl.* 2021;15(1):e2000040.

- 635 10. Musimbi ZD, Rono MK, Otieno JR, Kibinge N, Ochola-Oyier LI, de
636 Villiers EP, et al. Peripheral blood mononuclear cell transcriptomes
637 reveal an over-representation of down-regulated genes associated
638 with immunity in HIV-exposed uninfected infants. *Sci Rep.*
639 2019;9(1):18124.
- 640 11. Akat KM, Lee YA, Hurley A, Morozov P, Max KE, Brown M, et al.
641 Detection of circulating extracellular mRNAs by modified small-
642 RNA-sequencing analysis. *JCI Insight.* 2019;5(9).
- 643 12. Ji J, Chen R, Zhao L, Xu Y, Cao Z, Xu H, et al. Circulating exosomal
644 mRNA profiling identifies novel signatures for the detection of
645 prostate cancer. *Molecular Cancer.* 2021;20(1):58.
- 646 13. Tamura T, Yoshioka Y, Sakamoto S, Ichikawa T, and Ochiya T.
647 Extracellular vesicles as a promising biomarker resource in liquid
648 biopsy for cancer. *Extracellular Vesicles and Circulating Nucleic*
649 *Acids.* 2021;2(2):148.
- 650 14. Arroyo JD, Chevillet JR, Kroh EM, Ruf IK, Pritchard CC, Gibson DF, et
651 al. Argonaute2 complexes carry a population of circulating
652 microRNAs independent of vesicles in human plasma. *Proc Natl*
653 *Acad Sci U S A.* 2011;108(12):5003-8.
- 654 15. Turchinovich A, Weiz L, Langheinz A, and Burwinkel B.
655 Characterization of extracellular circulating microRNA. *Nucleic*
656 *Acids Res.* 2011;39(16):7223-33.
- 657 16. O'Grady T, Njock M-S, Lion M, Bruyr J, Mariavelle E, Galvan B, et al.
658 Sorting and packaging of RNA into extracellular vesicles shape
659 intracellular transcript levels. *BMC Biology.* 2022;20(1):72.
- 660 17. Payandeh Z, Tangruksa B, Synnergren J, Heydarkhan-Hagvall S,
661 Nordin JZ, Andaloussi SE, et al. Extracellular vesicles transport RNA
662 between cells: Unraveling their dual role in diagnostics and
663 therapeutics. *Mol Aspects Med.* 2024;99:101302.
- 664 18. Leidal AM, Huang HH, Marsh T, Solvik T, Zhang D, Ye J, et al. The
665 LC3-conjugation machinery specifies the loading of RNA-binding
666 proteins into extracellular vesicles. *Nat Cell Biol.* 2020;22(2):187-
667 99.

- 668 19. Kioko M, Mwangi S, Pance A, Ochola-Oyier LI, Kariuki S, Newton C,
669 et al. The mRNA content of plasma extracellular vesicles provides
670 a window into molecular processes in the brain during cerebral
671 malaria. *Science Advances*. 2024;10(33):eadl2256.
- 672 20. Yin H, Xie J, Xing S, Lu X, Yu Y, Ren Y, et al. Machine learning-based
673 analysis identifies and validates serum exosomal proteomic
674 signatures for the diagnosis of colorectal cancer. *Cell Reports
675 Medicine*. 2024;5(8).
- 676 21. Xu F, Wang K, Zhu C, Fan L, Zhu Y, Wang JF, et al. Tumor-derived
677 extracellular vesicles as a biomarker for breast cancer diagnosis
678 and metastasis monitoring. *iScience*. 2024;27(4).
- 679 22. DeMarino C, Denniss J, Cowen M, Norato G, Dietrich DK,
680 Henderson L, et al. HIV-1 RNA in extracellular vesicles is associated
681 with neurocognitive outcomes. *Nature Communications*.
682 2024;15(1):4391.
- 683 23. Gould SJ, Booth AM, and Hildreth JE. The Trojan exosome
684 hypothesis. *Proc Natl Acad Sci U S A*. 2003;100(19):10592-7.
- 685 24. Lenassi M, Cagney G, Liao M, Vaupotic T, Bartholomeeusen K,
686 Cheng Y, et al. HIV Nef is secreted in exosomes and triggers
687 apoptosis in bystander CD4+ T cells. *Traffic*. 2010;11(1):110-22.
- 688 25. Uemura T, Kawashima A, Jingushi K, Motooka D, Saito T, Nesrine S,
689 et al. Bacteria-derived DNA in serum extracellular vesicles are
690 biomarkers for renal cell carcinoma. *Heliyon*. 2023;9(9).
- 691 26. Stapleton JT, Xiang J, McLinden JH, Bhattarai N, Chivero ET,
692 Klinzman D, et al. A novel T cell evasion mechanism in persistent
693 RNA virus infection. *Trans Am Clin Climatol Assoc*. 2014;125:14-
694 24; discussion -6.
- 695 27. Price MA, Kilembe W, Ruzagira E, Karita E, Inambao M, Sanders EJ,
696 et al. Cohort Profile: IAVI's HIV epidemiology and early infection
697 cohort studies in Africa to support vaccine discovery. *Int J
698 Epidemiol*. 2021;50(1):29-30.
- 699 28. Hassan AS, Pybus OG, Sanders EJ, Albert J, and Esbjörnsson J.
700 Defining HIV-1 transmission clusters based on sequence data.
701 *Aids*. 2017;31(9):1211-22.

- 702 29. Kamali A, Price MA, Lakhi S, Karita E, Inambao M, Sanders EJ, et al.
703 Creating an African HIV clinical research and prevention trials
704 network: HIV prevalence, incidence and transmission. *PLoS One*.
705 2015;10(1):e0116100.
- 706 30. Tribolet L, Brice AM, Fulford TS, Layton DS, Godfrey DI, Bean AGD,
707 et al. Identification of a novel role for the immunomodulator ILRUN
708 in the development of several T cell subsets in mice.
709 *Immunobiology*. 2023;228(3):152380.
- 710 31. Samadi M, Salimi V, Haghshenas MR, Miri SM, Mohebbi SR, and
711 Ghaemi A. Clinical and molecular aspects of human pegiviruses in
712 the interaction host and infectious agent. *Virology Journal*.
713 2022;19(1):41.
- 714 32. Kioko M, Mwangi S, Pance A, Ochola-Oyier LI, Kariuki S, Newton C,
715 et al. The mRNA content of plasma extracellular vesicles provides
716 a window into molecular processes in the brain during cerebral
717 malaria. *Sci Adv*. 2024;10(33):eadl2256.
- 718 33. Kelley CF, Kraft CS, de Man TJ, Duphare C, Lee HW, Yang J, et al. The
719 rectal mucosa and condomless receptive anal intercourse in HIV-
720 negative MSM: implications for HIV transmission and prevention.
721 *Mucosal immunology*. 2017;10(4):996-1007.
- 722 34. Kelley CF, Pollack I, Yacoub R, Zhu Z, Van Doren VE, Gumber S, et
723 al. Condomless receptive anal intercourse is associated with
724 markers of mucosal inflammation in a cohort of men who have sex
725 with men in Atlanta, Georgia. *J Int AIDS Soc*. 2021;24(12):e25859.
- 726 35. Van Doren VE, Ackerley CG, Arthur RA, Murray PM, Smith SA, Hu YJ,
727 et al. Rectal mucosal inflammation, microbiome, and wound
728 healing in men who have sex with men who engage in receptive
729 anal intercourse. *Sci Rep*. 2024;14(1):31598.
- 730 36. Wacleche VS, Landay A, Routy J-P, and Ancuta P. The Th17 Lineage:
731 From Barrier Surfaces Homeostasis to Autoimmunity, Cancer, and
732 HIV-1 Pathogenesis. *Viruses*. 2017;9(10):303.
- 733 37. Matsushita K, Morrell CN, Cambien B, Yang SX, Yamakuchi M, Bao
734 C, et al. Nitric oxide regulates exocytosis by S-nitrosylation of N-
735 ethylmaleimide-sensitive factor. *Cell*. 2003;115(2):139-50.

- 736 38. Yazji I, Sodhi CP, Lee EK, Good M, Egan CE, Afrazi A, et al.
737 Endothelial TLR4 activation impairs intestinal microcirculatory
738 perfusion in necrotizing enterocolitis via eNOS-NO-nitrite
739 signaling. *Proc Natl Acad Sci U S A*. 2013;110(23):9451-6.
- 740 39. Good M, Sodhi CP, Yamaguchi Y, Jia H, Lu P, Fulton WB, et al. The
741 human milk oligosaccharide 2'-fucosyllactose attenuates the
742 severity of experimental necrotising enterocolitis by enhancing
743 mesenteric perfusion in the neonatal intestine. *Br J Nutr*.
744 2016;116(7):1175-87.
- 745 40. Shang Q, Bao L, Guo H, Hao F, Luo Q, Chen J, et al. Contribution of
746 glutaredoxin-1 to S-glutathionylation of endothelial nitric oxide
747 synthase for mesenteric nitric oxide generation in experimental
748 necrotizing enterocolitis. *Transl Res*. 2017;188:92-105.
- 749 41. Hosfield BD, Hunter CE, Li H, Drucker NA, Pecoraro AR, Manohar
750 K, et al. A hydrogen-sulfide derivative of mesalamine reduces the
751 severity of intestinal and lung injury in necrotizing enterocolitis
752 through endothelial nitric oxide synthase. *Am J Physiol Regul Integr*
753 *Comp Physiol*. 2022;323(4):R422-r31.
- 754 42. Zhang X, Tian B, Deng Q, Cao J, Ding X, Liu Q, et al. Nicotinamide
755 riboside relieves the severity of experimental necrotizing
756 enterocolitis by regulating endothelial function via eNOS
757 deacetylation. *Free Radic Biol Med*. 2022;184:218-29.
- 758 43. Li X, Bechara R, Zhao J, McGeachy MJ, and Gaffen SL. IL-17
759 receptor-based signaling and implications for disease. *Nat*
760 *Immunol*. 2019;20(12):1594-602.
- 761 44. Chao YY, Puhach A, Frieser D, Arunkumar M, Lehner L, Seeholzer T,
762 et al. Human T(H)17 cells engage gasdermin E pores to release IL-
763 1 α on NLRP3 inflammasome activation. *Nat Immunol*.
764 2023;24(2):295-308.
- 765 45. Wiche Salinas TR, Gosselin A, Raymond Marchand L, Moreira
766 Gabriel E, Tastet O, Goulet JP, et al. IL-17A reprograms intestinal
767 epithelial cells to facilitate HIV-1 replication and outgrowth in CD4+
768 T cells. *iScience*. 2021;24(11):103225.
- 769 46. Stieh DJ, Matias E, Xu H, Fought AJ, Blanchard JL, Marx PA, et al.
770 Th17 Cells Are Preferentially Infected Very Early after Vaginal

- 771 Transmission of SIV in Macaques. *Cell Host Microbe*.
772 2016;19(4):529-40.
- 773 47. El Hed A, Khaitan A, Kozhaya L, Manel N, Daskalakis D, Borkowsky
774 W, et al. Susceptibility of human Th17 cells to human
775 immunodeficiency virus and their perturbation during infection. *J*
776 *Infect Dis*. 2010;201(6):843-54.
- 777 48. McKinnon LR, Nyanga B, Chege D, Izulla P, Kimani M, Huibner S, et
778 al. Characterization of a human cervical CD4+ T cell subset
779 coexpressing multiple markers of HIV susceptibility. *J Immunol*.
780 2011;187(11):6032-42.
- 781 49. Moreno-Fernandez ME, Zapata W, Blackard JT, Franchini G, and
782 Chougnat CA. Human regulatory T cells are targets for human
783 immunodeficiency Virus (HIV) infection, and their susceptibility
784 differs depending on the HIV type 1 strain. *J Virol*.
785 2009;83(24):12925-33.
- 786 50. Jiao Y-M, Liu C-e, Luo L-J, Zhu W-J, Zhang T, Zhang L-G, et al.
787 CD4+CD25+CD127 regulatory cells play multiple roles in
788 maintaining HIV-1 p24 production in patients on long-term
789 treatment: HIV-1 p24-producing cells and suppression of anti-HIV
790 immunity. *International Journal of Infectious Diseases*. 2015;37:42-
791 9.
- 792 51. Ambrose RL, Liu YC, Adams TE, Bean AGD, and Stewart CR.
793 C6orf106 is a novel inhibitor of the interferon-regulatory factor 3-
794 dependent innate antiviral response. *J Biol Chem*.
795 2018;293(27):10561-73.
- 796 52. Lu B, Ren Y, Sun X, Han C, Wang H, Chen Y, et al. Induction of INK1T
797 by Viral Infection Negatively Regulates Antiviral Responses through
798 Inhibiting Phosphorylation of p65 and IRF3. *Cell Host & Microbe*.
799 2017;22(1):86-98.e4.
- 800 53. Ambrose RL, Brice AM, Caputo AT, Alexander MR, Tribolet L, Liu YC,
801 et al. Molecular characterisation of ILRUN, a novel inhibitor of
802 proinflammatory and antimicrobial cytokines. *Heliyon*.
803 2020;6(6):e04115.
- 804 54. Yu CF, Peng WM, Schlee M, Barchet W, Eis-Hübinger AM, Kolanus
805 W, et al. SOCS1 and SOCS3 Target IRF7 Degradation To Suppress

- 806 TLR7-Mediated Type I IFN Production of Human Plasmacytoid
807 Dendritic Cells. *J Immunol.* 2018;200(12):4024-35.
- 808 55. Kent SJ, and Kelleher AD. Expanding role for type I Interferons in
809 restricting HIV growth. *Immunol Cell Biol.* 2017;95(5):417-8.
- 810 56. Goodbourn S, Didcock L, and Randall RE. Interferons: cell
811 signalling, immune modulation, antiviral response and virus
812 countermeasures. *J Gen Virol.* 2000;81(Pt 10):2341-64.
- 813 57. Veazey RS, Pilch-Cooper HA, Hope TJ, Alter G, Carias AM, Sips M,
814 et al. Prevention of SHIV transmission by topical IFN- β treatment.
815 *Mucosal Immunol.* 2016;9(6):1528-36.
- 816 58. Roff SR, Noon-Song EN, and Yamamoto JK. The Significance of
817 Interferon- γ in HIV-1 Pathogenesis, Therapy, and Prophylaxis. *Front*
818 *Immunol.* 2014;4:498.
- 819 59. Zella D, Barabitskaja O, Burns JM, Romerio F, Dunn DE, Revello MG,
820 et al. Interferon-gamma increases expression of chemokine
821 receptors CCR1, CCR3, and CCR5, but not CXCR4 in monocytoid
822 U937 cells. *Blood.* 1998;91(12):4444-50.
- 823 60. Liptrott NJ, Egan D, Back DJ, and Owen A. IFN- γ 874A>T genotype is
824 associated with higher CCR5 expression in peripheral blood
825 mononuclear cells from HIV+ patients. *J Acquir Immune Defic*
826 *Syndr.* 2011;58(5):442-5.
- 827 61. Zhang W, Chen X, Gao G, Xing S, Zhou L, Tang X, et al. Clinical
828 Relevance of Gain- and Loss-of-Function Germline Mutations in
829 STAT1: A Systematic Review. *Front Immunol.* 2021;12:654406.
- 830 62. Erdős M, Jakobicz E, Soltész B, Tóth B, Bata-Csörgő Z, and Maródi
831 L. Recurrent, Severe Aphthous Stomatitis and Mucosal Ulcers as
832 Primary Manifestations of a Novel STAT1 Gain-of-Function
833 Mutation. *Front Immunol.* 2020;11:967.
- 834 63. Okada S, Asano T, Moriya K, Boisson-Dupuis S, Kobayashi M,
835 Casanova JL, et al. Human STAT1 Gain-of-Function Heterozygous
836 Mutations: Chronic Mucocutaneous Candidiasis and Type I
837 Interferonopathy. *J Clin Immunol.* 2020;40(8):1065-81.
- 838 64. Neupane B, Acharya D, Nazneen F, Gonzalez-Fernandez G, Flynt
839 AS, and Bai F. Interleukin-17A Facilitates Chikungunya Virus

- 840 Infection by Inhibiting IFN- α 2 Expression. *Front Immunol.*
841 2020;11:588382.
- 842 65. Zhang J, Liu K, Zhang G, Ling N, and Chen M. Interleukin-17A
843 pretreatment attenuates the anti-hepatitis B virus efficacy of
844 interferon-alpha by reducing activation of the interferon-
845 stimulated gene factor 3 transcriptional complex in hepatitis B
846 virus-expressing HepG2 cells. *Virology Journal.* 2022;19(1):28.
- 847 66. Yoon CH, Kim SY, Byeon SE, Jeong Y, Lee J, Kim KP, et al. p53-derived
848 host restriction of HIV-1 replication by protein kinase R-mediated
849 Tat phosphorylation and inactivation. *J Virol.* 2015;89(8):4262-80.
- 850 67. Wang X, Majumdar T, Kessler P, Ozhegov E, Zhang Y, Chattopadhyay
851 S, et al. STING Requires the Adaptor TRIF to Trigger Innate Immune
852 Responses to Microbial Infection. *Cell Host Microbe.*
853 2016;20(3):329-41.
- 854 68. Konkel JE, and Chen W. Balancing acts: the role of TGF- β in the
855 mucosal immune system. *Trends Mol Med.* 2011;17(11):668-76.
- 856 69. Biancheri P, Giuffrida P, Docena GH, MacDonald TT, Corazza GR,
857 and Di Sabatino A. The role of transforming growth factor (TGF)- β in
858 modulating the immune response and fibrogenesis in the gut.
859 *Cytokine Growth Factor Rev.* 2014;25(1):45-55.
- 860 70. Heitmann L, Rani R, Dawson L, Perkins C, Yang Y, Downey J, et al.
861 TGF- β -responsive myeloid cells suppress type 2 immunity and
862 emphysematous pathology after hookworm infection. *Am J Pathol.*
863 2012;181(3):897-906.
- 864 71. Andersson J, Boasso A, Nilsson J, Zhang R, Shire NJ, Lindback S, et
865 al. The prevalence of regulatory T cells in lymphoid tissue is
866 correlated with viral load in HIV-infected patients. *J Immunol.*
867 2005;174(6):3143-7.
- 868 72. Eggena MP, Barugahare B, Jones N, Okello M, Mutalya S, Kityo C, et
869 al. Depletion of regulatory T cells in HIV infection is associated with
870 immune activation. *J Immunol.* 2005;174(7):4407-14.
- 871 73. Jiang Q, Zhang L, Wang R, Jeffrey J, Washburn ML, Brouwer D, et al.
872 FoxP3+CD4+ regulatory T cells play an important role in acute HIV-

- 873 1 infection in humanized Rag2-/-gammaC-/- mice in vivo. *Blood*.
874 2008;112(7):2858-68.
- 875 74. Stapleton JT, Fong S, Muerhoff AS, Bukh J, and Simmonds P. The
876 GB viruses: a review and proposed classification of GBV-A, GBV-C
877 (HGV), and GBV-D in genus Pegivirus within the family Flaviviridae.
878 *J Gen Virol*. 2011;92(Pt 2):233-46.
- 879 75. Heringlake S, Ockenga J, Tillmann HL, Trautwein C, Meissner D,
880 Stoll M, et al. GB virus C/hepatitis G virus infection: a favorable
881 prognostic factor in human immunodeficiency virus-infected
882 patients? *J Infect Dis*. 1998;177(6):1723-6.
- 883 76. Nunnari G, Nigro L, Palermo F, Attanasio M, Berger A, Doerr HW, et
884 al. Slower progression of HIV-1 infection in persons with GB virus C
885 co-infection correlates with an intact T-helper 1 cytokine profile.
886 *Ann Intern Med*. 2003;139(1):26-30.
- 887 77. Tillmann HL, Heiken H, Knapik-Botor A, Heringlake S, Ockenga J,
888 Wilber JC, et al. Infection with GB virus C and reduced mortality
889 among HIV-infected patients. *N Engl J Med*. 2001;345(10):715-24.
- 890 78. Williams CF, Klinzman D, Yamashita TE, Xiang J, Polgreen PM,
891 Rinaldo C, et al. Persistent GB virus C infection and survival in HIV-
892 infected men. *N Engl J Med*. 2004;350(10):981-90.
- 893 79. Xiang J, Wünschmann S, Diekema DJ, Klinzman D, Patrick KD,
894 George SL, et al. Effect of coinfection with GB virus C on survival
895 among patients with HIV infection. *N Engl J Med*. 2001;345(10):707-
896 14.
- 897 80. Lalle E, Sacchi A, Abbate I, Vitale A, Martini F, D'Offizi G, et al.
898 Activation of interferon response genes and of plasmacytoid
899 dendritic cells in HIV-1 positive subjects with GB virus C co-
900 infection. *Int J Immunopathol Pharmacol*. 2008;21(1):161-71.
- 901 81. Carvalho T, Krammer F, and Iwasaki A. The first 12 months of
902 COVID-19: a timeline of immunological insights. *Nat Rev Immunol*.
903 2021;21(4):245-56.
- 904 82. Domizio JD, Gulen MF, Saidoune F, Thacker VV, Yatim A, Sharma K,
905 et al. The cGAS-STING pathway drives type I IFN immunopathology
906 in COVID-19. *Nature*. 2022;603(7899):145-51.

- 907 83. Scagnolari C, and Antonelli G. Type I interferon and HIV: Subtle
908 balance between antiviral activity, immunopathogenesis and the
909 microbiome. *Cytokine Growth Factor Rev.* 2018;40:19-31.
- 910 84. Su L. Pathogenic Role of Type I Interferons in HIV-Induced Immune
911 Impairments in Humanized Mice. *Curr HIV/AIDS Rep.*
912 2019;16(3):224-9.
- 913 85. Bhattarai N, McLinden JH, Xiang J, Landay AL, Chivero ET, and
914 Stapleton JT. GB virus C particles inhibit T cell activation via
915 envelope E2 protein-mediated inhibition of TCR signaling. *J*
916 *Immunol.* 2013;190(12):6351-9.
- 917 86. Maidana-Giret MT, Silva TM, Sauer MM, Tomiyama H, Levi JE,
918 Bassichetto KC, et al. GB virus type C infection modulates T-cell
919 activation independently of HIV-1 viral load. *Aids.*
920 2009;23(17):2277-87.
- 921 87. Chivero ET, Bhattarai N, McLinden JH, Xiang J, and Stapleton JT.
922 Human Pegivirus (HPgV; formerly known as GBV-C) inhibits IL-12
923 dependent natural killer cell function. *Virology.* 2015;485:116-27.
- 924 88. Kioko M, Pance A, Mwangi S, Goulding D, Kemp A, Rono M, et al.
925 Extracellular vesicles could be a putative posttranscriptional
926 regulatory mechanism that shapes intracellular RNA levels in
927 *Plasmodium falciparum*. *Nature Communications.*
928 2023;14(1):6447.
- 929 89. Rieckmann JC, Geiger R, Hornburg D, Wolf T, Kveler K, Jarrossay D,
930 et al. Social network architecture of human immune cells unveiled
931 by quantitative proteomics. *Nat Immunol.* 2017;18(5):583-93.
- 932 90. Febbo PG, Mulligan MG, Slonina DA, Stegmaier K, Di Vizio D,
933 Martinez PR, et al. Literature Lab: a method of automated literature
934 interrogation to infer biology from microarray analysis. *BMC*
935 *Genomics.* 2007;8:461.
- 936 91. Agrawal A, Balci H, Hanspers K, Coort SL, Martens M, Slenter DN,
937 et al. WikiPathways 2024: next generation pathway database.
938 *Nucleic Acids Res.* 2024;52(D1):D679-d89.